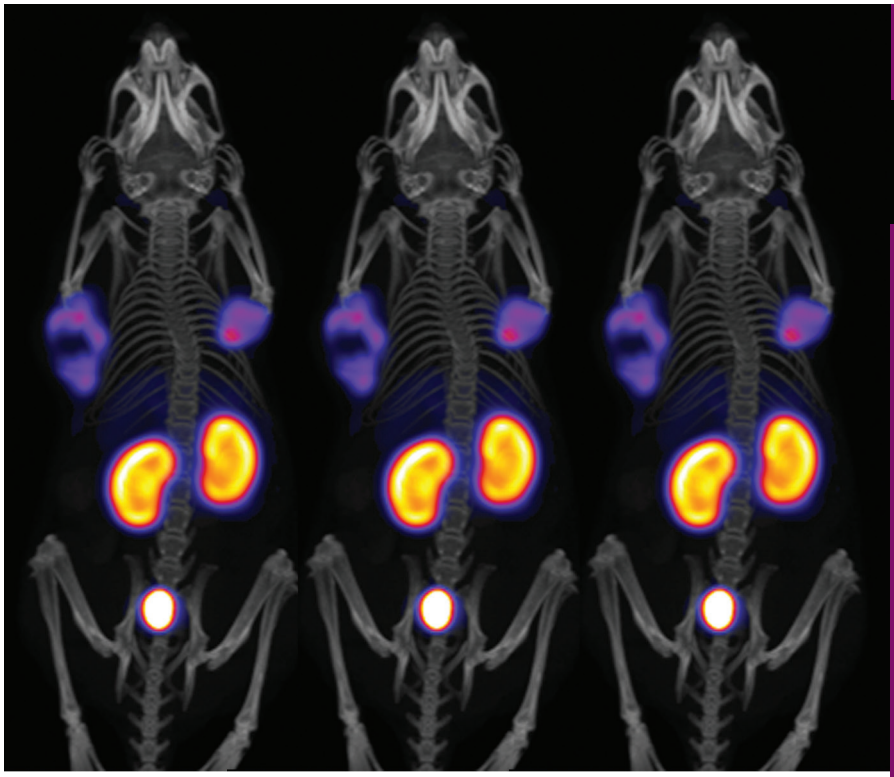

APPLICATION NOTE

Preclinical *In Vivo* Imaging

**Author:**

**Olivia J. Kelada, Ph.D.**

PerkinElmer, Inc.
Hopkinton,, MA

# Radiochemistry: PET Probe Development and Imaging

## Introduction

Positron Emission Tomography (PET) continues to be the primary functional imaging technique for conducting translational research studies aimed at identifying the molecular basis of human disease. This type of imaging would not be possible without the development of positron emitting radiotracers – the combination of a radionuclide with a biomolecule to target the pathway of interest. However, there are many challenges associated with radiolabeling. It is an expensive, highly-regulated and complex process that requires very specialized and inter-disciplinary knowledge. In addition, there are challenges associated with radiochemical yields, optimization of microfluidics and the chemical structures of imaging biomarkers. As a result, radiochemical yields are often low which can impact PET imaging, as generally PET scanners are not sensitive enough to detect low radiotracer activities.

PerkinElmer®
*For the Better*

With the highest sensitivity on the market, the G8 PET/CT can detect very low levels of radioactivity (Table 1), reducing the amount of activity that needs to be injected. This can alleviate the challenge of low PET probe yields and make it possible to image many biological pathways such as immune responses, where large doses of biomolecule or radioactivity could result in undesired therapeutic effects. An additional benefit is that lower amounts of probes are required to be synthesized, allowing for a more efficient use of resources, reduced procurement expenses and lower waste storage and disposal fees.

## How PET Detector Sensitivity is Increased

The high PET sensitivity (~14% uniform sensitivity across the FOV) of the G8 is made possible through a) High atomic number (Z=83) of the BGO crystal detectors as this increases the probability of a photoelectric event at the first interaction site b) The arrangement of the four panel detector heads as they are placed close together (unlike the classic ring design) thus closer to the animal and emitted photons and c) Improved crystal cutting that reduces the gaps between adjacent crystals and increases the packing fraction. In addition, to achieve equivalent sensitivity on a

*Table 1.* Data demonstrates the low radiotracer activities that can imaged on the G8 PET/CT.

| Author | G4 or G8 | Radiotracer | Lowest activity used (uCi) | (MBq) | Application* |
|---|---|---|---|---|---|
| Bansal et al. 2015 | G4 | $^{89}$Zr(HPO4)2, $^{89}$Zr-labeled hMSCs | 2.00 | 0.07 | Novel $^{89}$Zr cell labeling PET cell tracking |
| Gu et al. 2013 | G4 | $^{64}$Cu-minibody, $^{18}$F-FDG | 3.70 | 0.14 | Performance testing of high sensitivity PET Imaging system |
| Yang et al. 2016 | G4 | $^{89}$Zr(HPO4)2, $^{89}$Zr-labeled hMSCs | 7.50 | 0.28 | PET tracking to determine therapeutic value of human adipose tissue in AVF |
| Haller et al. 2015 | G4 | $^{18}$F-AzaFol, $^{18}$F-fallypride | 10.0 | 0.37 | Chick and mouse comparison for PET probe uptake and stability |
| Meimetis et al. 2015 | G4 | $^{89}$Zr-DFO-BODIPY-trastuzumab | 10.0 | 0.37 | Multimodal imaging of antibodies with PET |
| Boros et al. 2016 | G4 | $^{89}$Zr–L4/L5, $^{89}$Zr-DFO | 10.0 | 0.37 | Novel immunoconjugation of $^{89}$Zr for PET |
| Peng et al. 2014 | G4 | $^{11}$C-PBR28 | 13.0 | 0.48 | PET to investigate role of acetyl-coA in neurodegeneration |
| Lazari et al. 2014 | G4 | $^{18}$F-FLT, $^{18}$F-FDG,$^{18}$F-fallypride | 20.0 | 0.74 | Fully automated production of diverse $^{18}$F-labeled PET tracers |
| Evdokimov et al. 2014 | G4 | $^{18}$F-FMT | 20.0 | 0.74 | Development of novel CNS PET probe |
| Faltermeier et al. 2015 | G4 | $^{18}$F-FDG | 20.0 | 0.74 | PET imaging to identify kinases driving prostate cancer metastasis |
| Evdokimov et al. 2015 | G4 | $^{18}$F-2-DFR, $^{18}$F-DFA | 20.0 | 0.74 | Development of PET probe for liver function imaging |
| Kim et al. 2016 | G4 | $^{18}$F-CFA | 20.0 | 0.74 | Development of a PET probe for deoxycytidine kinase activity imaging |
| Hermann et al. 2013 | G4 | $^{18}$F-FDG | 25.0 | 0.93 | Evaluation of a bench-top preclinical PET scanner |
| Lozier et al. 2015 | G4 | $^{18}$F-FDG | 25.0 | 0.93 | Assessment of LIN28 oncogenic driver in neuroblastoma using PET |
| van der Meulen et al. 2015 | G4 | $^{44}$Sc-DOTANOC | 27.0 | 1.00 | Evaluation of $^{44}$Sc biodistribution in vivo with PET |
| Boschi et al. 2016 | G8 | $^{18}$F-PSMA-11 | 38.0 | 1.40 | Synthesis and preclinical evaluation of an Al$^{18}$F radiofluorinated PSMA ligand |
| Seo et al. 2015 | G4 | $^{64}$Cu-NOTA-UCNPs | 40.0 | 1.48 | Assessment of radiolabeled upconverting nanoparticles with PET |
| Witney et al. 2014 | G4 | $^{18}$F-FPIA | 50.0 | 1.85 | Preclinical evaluation of a novel PET imaging agent for tumor detection |
| Song et al. 2016 | G4 | $^{18}$F-FMISO | 50.0 | 1.85 | PET to assess oxygen changes after high-dose radiation therapy |
| van Elssen et al. 2017 | G8 | $^{64}$Cu-VHH4 | 50.0 | 1.85 | Imaging of human immune responses in a human xenograft model of graft vs host disease |
| Mueller et al. 2016 | G8 | $^{152}$Tb-DOTANOC | 90.0 | 3.33 | $^{152}$Tb-DOTANOC for PET radiolanthanide imaging |
| Farkas et al. 2016 | G8 | $^{64}$Cu- and $^{68}$Ga-labeled NODAGA-folate | 94.0 | 3.48 | $^{64}$Cu- and $^{68}$Ga-Based PET Imaging of folate receptor-positive tumors |
| Jang et al. 2013 | G4 | $^{64}$Cu-Sar-chTNT-3 | 100 | 3.70 | PET to assess the use of chemotherapy to improve the biodistribution of antibodies |
| Hu et al. 2015 | G4 | $^{18}$F-FDG | 100 | 3.70 | Nanoparticle-mediated radiopharmaceutical-excited fluorescence in vivo imaging |
| Umbricht et al. 2017 | G8 | $^{44}$Sc-PSMA-617, $^{68}$Ga-PSMA-11, $^{68}$Ga-PSMA-617 | 135** | 5.00 | $^{44}$Sc-PSMA-617 for radiotheragnostics in comparison with $^{68}$Ga-PSMA ligands |
| Mueller et al. 2016 | G8 | $^{149}$Tb-DOTANOC | 190** | 7.03 | Alpha-PET with terbium-149 in mice |
| Domnanich et al. 2016 | G8 | $^{44}$Sc/$^{68}$Ga-labeled DOTA/NODAGA peptides | 270** | 9.99 | $^{44}$Sc for labeling of DOTA- and NODAGA peptides |
| Moon et al. 2015 | G4 | $^{68}$Ga-DOTA-IO-GUL | 276** | 10.2 | Development of PET/MR probe for PSMA targeting |

* All studies conducted in mice

** Due to tracer half-life and study design higher activities were injected prior to imaging

BGO crystal detector system, lower detector thickness is required, leading to reduced parallax errors and better spatial resolution.

## Translational Research Benefits from Imaging Low Radiotracer Activities

Mice are approximately 3000 times smaller in mass and volume than humans. To obtain preclinical PET images of comparable statistical quality to clinical ones, the number of counts per voxel (which is inversely proportional to voxel volume) can either be compensated by increasing the radioactivity of injected probes or by improving the sensitivity of the scanner. However, for preclinical imaging, the typical amount of radioactivity administered is 7.4 MBq (200 µCi). This delivers a much higher dose per gram of tissue than in humans (typical administered activity of 370 MBq (10 mCi)). The higher absorbed dose can lead to biological effects such as stimulated cell proliferation, induced radio-resistance and elevated gene expression. Such biological effects may interfere and bias the results in pharmaceutical and genetic studies, leading to discrepancies in translational research between mouse models and clinical applications. This may be even more important for longitudinal studies that require serial imaging. Also, for many applications, signal uptake can be limited by the number of binding sites available, thus when higher activity of radiotracer (and in turn higher amounts of targeting agent) are injected, this may block the binding receptors and prevent repeated imaging. The amount of injected probe should be below levels that perturb the in vivo system and this may limit the amount of radioactivity that can be injected into the animal. Thus, a preclinical PET scanner with high sensitivity lowers the activities of radioisotopes that are needed to obtain high quality PET images. In turn, this results in less exposure to the animal and the investigator. For biodistribution studies on the G8, the typical administered radioactivity amount should be less than 1.5 MBq (40 µCi), which is five times lower than established procedures and is potentially more physiologically relevant[1].

## Novel Radiotracer Development Using the G8 PET/CT

Figure 1 shows images of newly developed tracers using the G8 PET/CT.

**Panel a** $^{64}$Cu-rf42 (an albumin binding NODAGA-folate) showed much better resolution than $^{68}$Ga-rf42 of tumor xenografts and kidneys in CD1 nude mice with KB tumor xenografts and SCID mouse with a LNCaP tumor xenografts. The image shows a 10 min static scan of 4.3 MBq (116.2 uCi) and standard CT. The data suggests that $^{64}$Cu-rf42 is a more favorable PET agent due to improved tumor-to-kidney ratios and the more physiologically suitable half-life of $^{64}$Cu as it matches the circulation time of the albumin binding NODAGA–folate and allows for serial PET imaging at later time points which is not possible when using $^{68}$Ga[2].

**Panel b** $^{18}$F-AzaFol ($^{18}$F-labeled folate-based radiotracer) shows specificity in both the tumor and kidneys in CD1 nude mice with KB tumor xenografts. The image shows a 10 min static scan of 2.1 MBq (56.8 uCi) and standard CT. Results suggested that $^{18}$F-AzaFol is an appropriate tool for imaging FR-positive tumors[3].

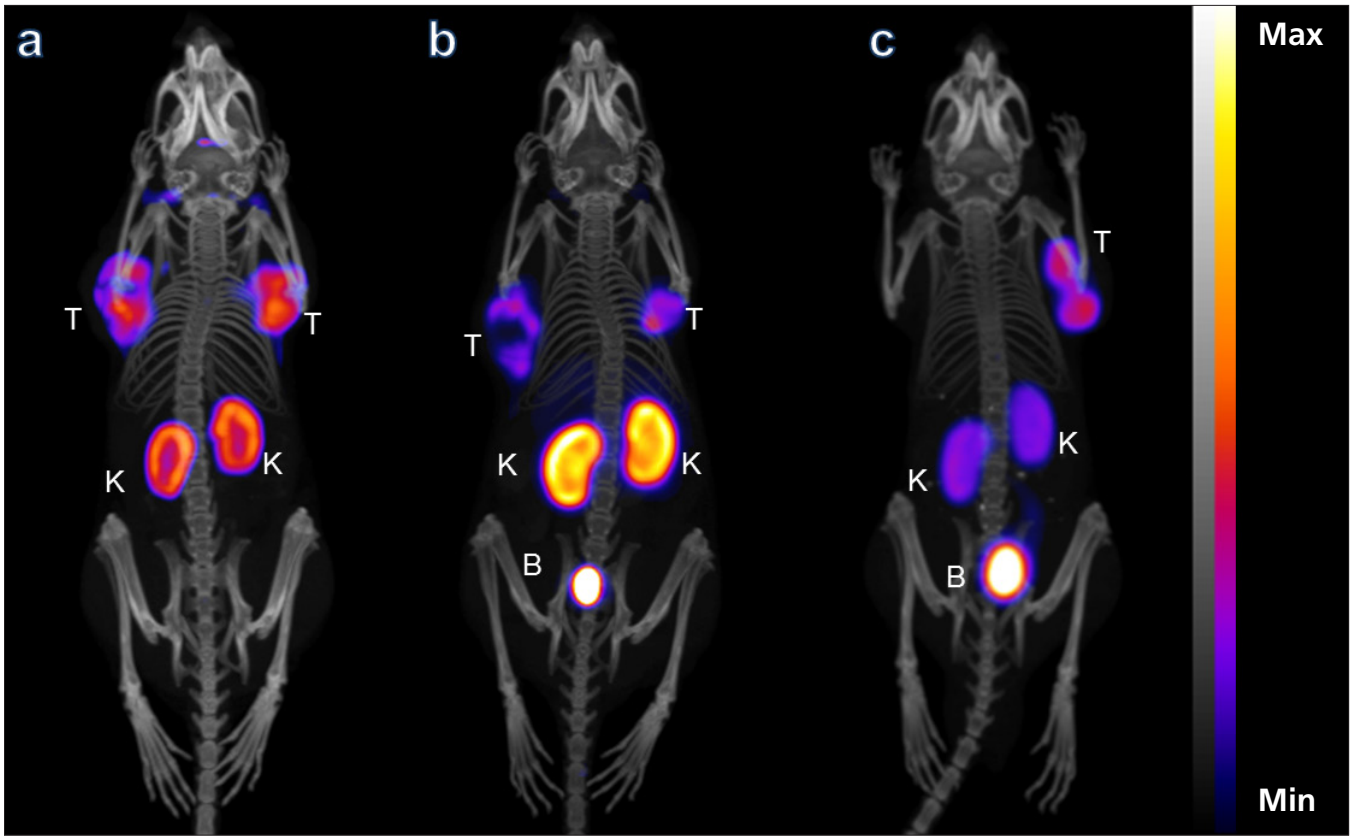


*Figure 1.* $^{64}$Cu-NODAGA-folate static PET scan in CD1 nude mice with cervical cancer xenografts (b) $^{18}$F-AzaFol static PET in CD1 nude mice with cervical cancer xenografts (c) $^{44}$Sc labeled PSMA-617 static PET/CT scan of SCID mouse with LNCaP prostate cancer xenograft T = Tumor, K = Kidney and B = Bladder
All PET/CT images courtesy of Dr. Cristina Müller Center for Radiopharmaceutical Sciences (ETH/PSI), Zurich, Switzerland and used with permission.

## PET Probe Development and Imaging on the G8 PET/CT: Customer Testimonial

**Dr. Cristina Müller Center for Radiopharmaceutical Sciences (ETH/PSI), Zurich, Switzerland**

"The G8 PET/CT was installed at the Center for Radiopharmaceutical Sciences ETH-PSI in 2015. It has proven to be particularly effective for the evaluation of novel in-house produced radiotracers, that are initially only available in small quantities. The fact that the scanner is small and mobile has allowed us to transport it to other facilities including the Center for Proton Therapy located at the PSI where the G8 scanner was used for imaging in vivo $^{11}$C production after proton irradiation of tumor xenografts in mice."

**Panel c** $^{44}$Sc labeled PSMA-617 shows specificity and sensitivity in SCID mouse with LNCaP tumor xenografts. The image shows a 10 min static scan of 0.8 MBq and standard CT. Due to the desirable nearly four-fold longer half-life of $^{44}$Sc compared to $^{68}$Ga, the feasibility of centralized production of $^{44}$Sc and transport to satellite PET centers, $^{44}$Sc -PSMA-617 is appealing for clinical PET imaging of prostate cancer patients[4].

## Summary

With the highest sensitivity on the market, the preclinical G8 PET/CT can detect very low levels of radioactivity. This is ideal for PET probe development, where yields are often low, and studies investigating various applications where large doses of carrier or radioactivity could elicit unexpected biological effects or block the binding sites and prevent repeated imaging. The amount of injected probe should be below levels that perturb the in vivo system and this may limit the amount of radioactivity that can be injected into the animal. The G8 PET/CT facilitates imaging with more translation doses. This, in combination with its small footprint, makes it the ideal tool for the advancement of novel PET radiotracer development and imaging.

## References


1. Gu Z, et al. NEMA NU-4 performance evaluation of PETbox4, a high sensitivity dedicated PET preclinical tomograph. Phys Med Biol. 2013; 58:3791-814.
2. Farkas R, et al. 64Cu- and 68Ga-Based PET Imaging of Folate Receptor-Positive Tumors: Development and Evaluation of an Albumin-Binding NODAGA–Folate. Mol. Pharmaceutics 2016, 13,1979-87.
3. Betzel T, et al. Radiosynthesis and Preclinical Evaluation of 3′-Aza-2′-[18F]fluorofolic Acid: A Novel PET Radiotracer for Folate Receptor Targeting. Bioconjug Chem 2013, 24, 205-14.
4. Umbricht CA, et al. 44Sc-PSMA-617 for radiotheragnostics in tandem with 177Lu-PSMA-617 - preclinical investigations in comparison with 68Ga-PSMA-11 and 68Ga-PSMA-617. EJNMMI Research 2017, 7:9.



**PerkinElmer, Inc.**
940 Winter Street
Waltham, MA 02451 USA
P: (800) 762-4000 or
(+1) 203-925-4602
**www.perkinelmer.com**


PerkinElmer®




013483_01 PKI